ELSEVIER

Study of the bonding properties of the bis[2-(3,5-dimethyl-1-pyrazolyl)ethyl]ether toward Rh(I): an hemilabile ligand exhibiting κ^3N,N,O meridional or facial coordination mode

Anna Boixassa [a], Josefina Pons [a], Josep Ros [a,*], René Mathieu [b,*], Noël Lugan [b]

[a] *Departament de Química, Unitat de Química Inorgànica, Facultat de Ciències, Universitat Autònoma de Barcelona, 08193 Bellaterra-Cerdanyola, Barcelona, Spain*
[b] *Laboratoire de Chimie de Coordination du CNRS, 205 Route de Narbonne, 31077 Toulouse Cedex 4, France*

Abstract

The bis[2-(3,5-dimethyl-1-pyrazolyl)ethyl]ether ligand (L_1) reacts with $[Rh(COD)(THF)_2][BF_4]$ generated in situ, giving $[Rh(COD)(L_1\text{-}\kappa^2N,N)][BF_4]$ ($[1][BF_4]$). The 1,5-cyclooctadiene ligand is displaced by carbon monoxide to generate $[Rh(CO)_2(L_1)][BF_4]$ ($[2][BF_4]$) in which in the solid state, the ligand L_1 adopts a facial κ^3N,N,O bonding mode. This is the first example of such a coordination mode for this ligand, which generally prefers a 'T-shaped' meridional bonding mode. In solution $[2][BF_4]$ exists as a mixture of two isomers in rapid equilibrium on the NMR time scale, $[Rh(CO)_2(L_1\text{-}\kappa^2N,N)]^+$ ($[2a]^+$) and the major compound $[Rh(CO)_2(L_1\text{-}\kappa^3N,N,O)]^+[2b]^+$. $[2][BF_4]$ looses easily one molecule of carbon monoxide at room temperature leading to $[Rh(CO)(L_1\text{-}\kappa^3N,N,O)][BF_4]$ ($[3][BF_4]$) in which L_1 adopts a 'T-shaped' meridional bonding mode. Carbon monoxide addition in solution regenerates rapidly $[2][BF_4]$. The single-crystal X-ray structures of $[1][BF_4]$, $[2b][BF_4]$ and $[3][BF_4]$ are reported.
© 2003 Elsevier B.V. All rights reserved.

Keywords: Rhodium(I) complexes; Ether–pyrazole ligand; Hemilabile ligand; Tridentate ligand

1. Introduction

In a recent publication some of us have shown that the bis[2-(3,5-dimethyl-1-pyrazolyl)methyl]ethylamine (**L**) is a very flexible ligand in Rh(I) complexes, through the possibility of κ^2N,N or κ^3N,N,N bonding mode depending on the electronic configuration and the steric constraints around the metal [1]. The hemilabile centre of the ligand is logically, the nitrogen atom of the amine function. As an extension of that work, it was tempting to consider ligands similar to **L**, but containing a harder donor centre than the nitrogen atom of the amine group, such as the oxygen of an ether group, and to investigate

the incidence of such a modification on the bonding properties of the ligand.

Most of known ligands associating pyrazole rings and one (or more) ether groups consist of two pyrazolyl rings linked together through both N1 atoms by an ether or a polyether chain [2,3]. These ligands were mainly designed for the capture and selective complexation of alkaline, ammonium or calcium cations. The bis[2-(3,5-dimethyl-1-pyrazolyl)ethyl]ether (**L₁**, Fig. 1) has retained our attention. Its coordination chemistry involving first and second row metals such as Cu(I) [4], Co(II) [5] and Cd(II) [6] has been studied and in all cases the ligand has been shown to adopt a meridional κ^3 bonding mode. For our part, we have investigated the bonding properties of the ligand **L₁** toward Rh(I), which is a softer metallic centre, and in the present paper we disclose the synthesis, the behaviour in solution and the crystal structures of $[Rh(COD)(L_1\text{-}\kappa^2N,N)][BF_4]$ ($[1][BF_4]$), $[Rh(CO)_2(L_1\text{-}\kappa^2N,N,)][BF_4]$ ($[2][BF_4]$) and

* Corresponding authors. Tel.: +33-5-6133-3183; fax: +33-5-6155-3003.
E-mail addresses: josep.ros@uab.es (J. Ros), mathieu@lcc-toulouse.fr (R. Mathieu).
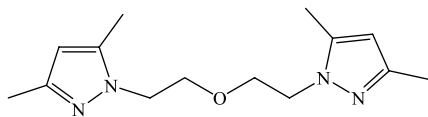
Fig. 1. Structure of the bis[2-(3,5-dimethyl-1-pyrazolyl)ethyl]ether ligand (**L₁**).

$[Rh(CO)(L_1\text{-}\kappa^3 N,N,O)][BF_4]$ ([**3**][BF₄]) complexes (COD = 1,5-cyclooctadiene).

2. Results and discussion

The bis[2-(3,5-dimethyl-1-pyrazolyl)ethyl]ether reacts at room temperature with [Rh(COD)(THF)₂][BF₄], generated in situ from the reaction of [Rh(COD)Cl]₂ and AgBF₄ in THF, to give the complex [Rh(COD)(L₁-$\kappa^2 N,N$)][BF₄] ([**1**][BF₄]) in 87% yield. This complex, which crystallizes as yellow needles, was characterised by elemental analyses and spectroscopic methods. At room temperature, the compound shows a well resolved but complex ¹H NMR spectrum. Signals assigned to the olefinic protons of the cyclooctadiene ligand are observed at 3.90 and 3.71 ppm as two broad peaks in a 1:1 ratio. These chemical shifts are in full agreement with the presence of nitrogen atoms in a *trans* position [1]. The non-equivalence of the olefinic hydrogens atoms reveals a rigid conformation of the bonded ligand L₁. Corroborating the rigidity of the ligand, the methylene protons of the OCH₂CH₂N chain exhibit a diastereotopic character and appear as three groups of signals at 4.26, 4.48 and 6.28 ppm, which integrate as 4, 2 and 2 protons. The spin system, which can be analysed as two identical AA'BB' spin systems, has been simulated using the gNMR program [7]. Finally, the pyrazolic methyl and CH groups give singlets at 2.21, 2.80 and 5.93 ppm, respectively. From these data it was not possible, however, to ascertain whether the ligand **L₁** in [**1**]⁺ was $\kappa^2 N,N$ or $\kappa^3 N,N,O$ bonded to rhodium. The structure of [**1**][BF₄] was further investigated in the solid state by X-ray diffraction.

The complex crystallizes with two independent ion pairs per unit cell. The two cations [**1**]⁺ present the same geometry, all the corresponding distances and angles being equal within the experimental errors. A perspective view of one of the two independent cations [**1**]⁺ (cation A) is shown on Fig. 2. Selected bond lengths and angles are provided in Table 1. The distance between the rhodium and the oxygen atom (Rh(1A)–O(8A) = 4.146(5) Å; Rh(1B)–O(8B) = 4.145(5) Å) is clearly longer than the sum of the van der Waals radii (3.37 Å), probing that there is no interaction between the two atoms. The rhodium atom is located slightly above the mean plane defined by the two pyrazolic nitrogen atoms and the centroid of the C=C bonds (0.021 Å for molecule A, 0.029 Å for molecule B). The Rh–N
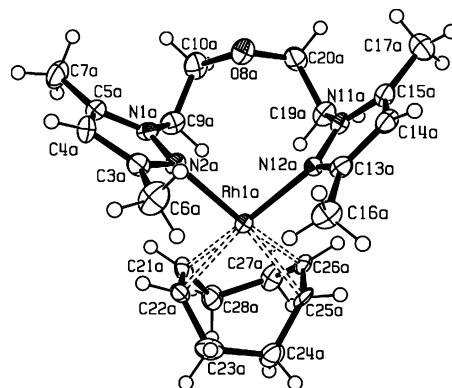

Fig. 2. Crystal structure of the cation [**1**]⁺ showing the numbering scheme; ellipsoids are drawn at the 30% probability level.

Table 1
Selected bond lengths (Å) and bond angles (°) for [**1**][BF₄], [**2b**][BF₄] and [**3**][BF₄]

	[**1**][BF₄] Molecule A	[**1**][BF₄] Molecule B	[**2b**][BF₄]	[**3**][BF₄]
Bond lengths				
C(21)–C(22)	1.377(8)	1.410(9)		
C(25)–C(26)	1.415(8)	1.370(8)		
C(21)–Rh(1)	2.151(5)	2.1285)		
C(22)–Rh(1)	2.150(5)	2.167(5)		
C(25)–Rh(1)	2.172(5)	2.148(5)		
C(26)–Rh(1)	2.142(5)	2.165(5)		
N(2)–Rh(1)	2.128(5)	2.138(5)	2.1264(19)	2.032(4)
N(12)–Rh(1)	2.145(5)	2.141(5)	2.1033(19)	2.042(4)
C(1)–Rh(1)			1.843(3)	1.795(5)
C(2)–Rh(1)			1.856(2)	
O(8)–Rh(1)	4.146(5)	4.146(5)	2.764(2)	2.116(3)
Bond angles				
C(10)–O(8)–C(20)	116.6(5)	116.1(5)	113.13(16)	113.2(4)
C(10)–O(8)–Rh(1)				123.4(3)
C(20)–O(8)–Rh(1)				123.4(3)
C(21)–Rh(1)–C(25)	89.7(2)	97.0(2)		
C(21)–Rh(1)–C(26)	81.8(2)	81.7(2)		
C(22)–Rh(1)–C(25)	81.3(2)	80.8(2)		
C(22)–Rh(1)–C(26)	97.3(2)	89.2(2)		
C(21)–Rh(1)–N(2)	90.0(2)	87.9(2)		
C(22)–Rh(1)–N(2)	88.0(2)	91.5(2)		
C(25)–Rh(1)–N(2)	162.6(2)	160.0(2)		
C(26)–Rh(1)–N(2)	158.2(2)	162.3(2)		
C(21)–Rh(1)–N(12)	166.4(2)	161.4(2)		
C(22)–Rh(1)–N(12)	156.0(2)	159.9(2)		
C(25)–Rh(1)–N(12)	91.5(2)	88.30(2)		
C(26)–Rh(1)–N(12)	90.8(2)	92.2(2)		
N(2)–Rh(1)–N(12)	92.8(2)	93.2(2)	90.03(7)	173.2(2)
N(2)–Rh(1)–O(8)			83.40(8)	86.5(2)
N(12)–Rh(1)–O(8)			80.47(8)	86.8(2)
C(1)–Rh(1)–O(8)				179.0(2)
C(2)–Rh(1)–O(8)				
C(1)–Rh(1)–N(12)			91.91(9)	92.7(2)
C(2)–Rh(1)–N(2)			87.83(9)	
C(1)–Rh(1)–N(2)			166.49(10)	94.1(2)
C(2)–Rh(1)–N(12)			177.77(8)	
C(1)–Rh(1)–C(2)			90.02(10)	

distances are equal within the experimental errors and with an average value of 2.14 Å, they are slightly longer than those found in related complexes associating bis(pyrazolyl)alkylamines [1], bis(pyrazolyl)alkanes [8], tris(pyrazolyl)alkanes [9], or tris(pyrazolyl)hydridoborate [10,11] to rhodium (2.082 < Rh–N < 2.133 Å).

It thus appears that, by contrast to the ligand bis[(3,5-dimethyl-1-pyrazolyl)methyl]ethylamine ligand **L** in [Rh(COD)(L-$\kappa^3 N,N,N$)][BF$_4$] [1], the ligand **L$_1$** in [**1**]$^+$ adopts a $\kappa^2 N,N$ bonding mode.

In order to evaluate further the coordination properties of **L$_1$** toward a rhodium(I) centre of different steric and electronic environment, the 1,5-cyclooctadiene in [**1**]$^+$ was substituted for carbon monoxide. This was readily achieved by bubbling carbon monoxide through a solution of [**1**][BF$_4$] in dichloromethane at room temperature to give [Rh(CO)$_2$(**L$_1$**)][BF$_4$] ([**2**][BF$_4$]). The IR spectrum of [**2**]$^+$ in solution shows four bands in the νCO region, two weak bands at 2105 and 2042 cm^{-1} and two strong bands at 2090 and 2022 cm^{-1}, suggesting the presence of two isomers in solution, namely [**2a**]$^+$ for the minor complex, and [**2b**]$^+$ for the major one. Similar observations have been made in the case of [Rh(CO)$_2$(**L**)][BF$_4$] and it was shown that the weakest bands correspond to the isomer in which the ligand **L** was $\kappa^2 N,N$-bonded to rhodium [1]. As the CO absorption bands of a given 18 valence electron complex are expected to appear at lower frequencies as compared to a 16 electron one, it can be deduced that in the major isomer, [**2b**][BF$_4$], the oxygen of the ether group is bonded to rhodium. Suitable crystals for X-ray diffraction of [**2**][BF$_4$] were obtained by crystallisation under a CO atmosphere. Infrared spectrum in KBr dispersion showed that these crystals corresponded to the major isomer of [**2**][BF$_4$], [**2b**][BF$_4$] (νCO: 2082, 2009 cm^{-1}). Fig. 3 depicts cation [**2b**]$^+$. Selected bond lengths and angles are collected in Table 1. The complex [**2b**]$^+$ presents a distorted square pyramid geometry around rhodium: the nitrogen atoms N(2) and N(12) of the pyrazolyl ligands and the two carbons atoms C(1) and C(2) of the carbonyl ligands constitute the basis of the
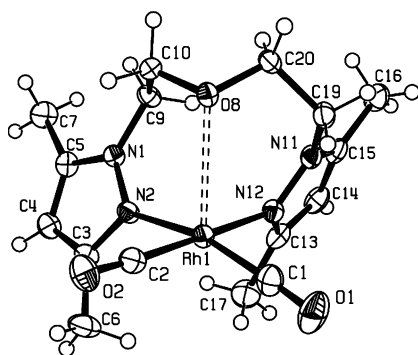
pyramid, while the oxygen atom O(8) of the ether arm figures its summit. The rhodium atom lays 0.122 Å out of basis of the pyramid, toward the oxygen atom O(8). The Rh–O(8) distance of 2.764(2) Å is shorter than the sum of the van der Waals radii (3.37 Å) and this is consistent with a bonding interaction between the two atoms. It is worth noting, however, this Rh–O bond is one of the longest reported so far [12]. Due to the steric strains, the Rh–O(8) bond is bent over the ligand **L$_1$** (O(8)–Rh–N(2) = 83.40(8)°, O(8)–Rh–N(12) = 80.43(8)°). It thus appears that in the solid state the ligand **L$_1$** adopts a facial $\kappa^3 N,N,O$ bonding mode. This is the first example of such a coordination mode for this ligand, which generally prefers a 'T-shaped' meridional coordination mode [5].

The ^{1}H NMR spectrum of [**2**]$^+$ at 295K shows sharp resonances for the CH and CH$_3$ groups of the pyrazolyl cycles but ill defined broad signals in the region where the methylene resonances are expected (4–5 ppm). This suggests the occurrence of a fluxional process, which was investigated further by variable-temperature ^{1}H-NMR experiments at 500 MHz. At 240 K the signals of the methylene protons are well defined giving an AA′BB′ spin system at 4.87 and 4.09 ppm, and 4.21 and 3.99 ppm, respectively (Fig. 4). Coupling constants and chemical shifts have been determined by comparing the ^{1}H-NMR spectrum of this region with a simulated spectrum using the gNMR program [7]. Besides the CH and CCH$_3$ groups of the pyrazolyl cycles are not significantly affected and their resonances remain as singlet upon cooling. Lowering the temperature does not

Fig. 3. Crystal structure of the cation [**2b**]$^+$ showing the numbering scheme; ellipsoids are drawn at the 30% probability level.
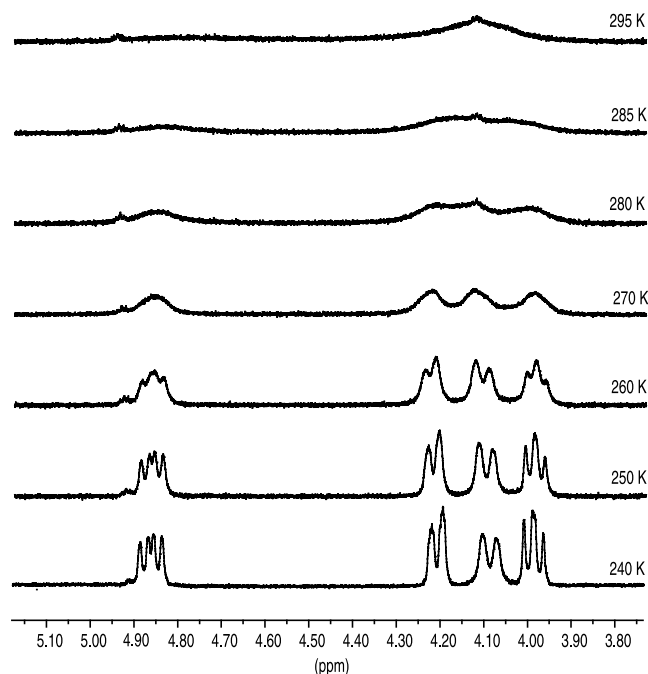

Fig. 4. 500 MHz ^{1}H-NMR variable temperature spectra (from 295 to 240 K) of the methylene region of cation [**2**]$^+$ in (CD$_3$)$_2$CO solution.

induce further significant change, except a slight broadening of the methylene resonances. These observations are consistent with a reversible opening of the Rh–O bond and imply, in accordance with the IR data, the existence in solution of both $[Rh(CO)_2(\mathbf{L_1}\text{-}\kappa^2N,N)]^+$ $([\mathbf{2a}]^+)$ and $[Rh(CO)_2(\mathbf{L_1}\text{-}\kappa^3N,N,O)]^+$ $[\mathbf{2b}]^+$ species in solution in a fast (NMR-time scale) equilibrium (Scheme 1). However, at 240 K the concentration of $[\mathbf{2a}]^+$ is certainly low as it has not been clearly detected by NMR.

Attempts to crystallize $[\mathbf{2}][BF_4]$ under a nitrogen atmosphere led to $[Rh(CO)(\mathbf{L_1}\text{-}\kappa^3N,N,O)][BF_4]$ $([\mathbf{3}][BF_4])$ in a nearly quantitative yield. Noticeably, this shows that $[\mathbf{2}][BF_4]$ is more easily decarbonylated than the parent complex $[Rh(CO)_2(\mathbf{L}\text{-}\kappa^3N,N,N)][BF_4]$ as the later species requires refluxing conditions in THF to give $[Rh(CO)(\mathbf{L}\text{-}\kappa^3N,N,N)][BF_4]$ [1]. Bubbling carbon monoxide through a solution of $[\mathbf{3}][BF_4]$ regenerates quantitatively $[\mathbf{2}][BF_4]$ (Scheme 2). The infrared spectrum of $[\mathbf{3}][BF_4]$ in dichloromethane solution shows a νCO absorption at 1994 cm^{-1}.

The solid state structure of $[\mathbf{3}]^+$ is shown on Fig. 5. Bond lengths and angles of interest are gathered in Table 1. The cation $[\mathbf{3}]^+$ exhibits a square planar geometry around Rh. Like in the known Cu(I), and Cd(II) complexes the ligand $\mathbf{L_1}$ adopts a 'T-shaped' coordination mode with a N(2)–Rh–N(12) angle of 173.2(2)°. The Rh–O(8) bond distance of 2.116(3) Å is very similar to the corresponding Rh–O bond distance in the related species $[Rh(CO)(Ph_2P(CH_2)_2O(CH_2)_2PPh_2)][PF_6]$ (2.112(8) Å) [13]. The Rh–N bond distances are significantly shorter than in $[\mathbf{1}]^+$ and $[\mathbf{2b}]^+$ but compares well with the corresponding Rh–N bond distances found in $[Rh(CO)_2(\mathbf{L}\text{-}\kappa^3N,N,N)][BF_4]$ [1]. Finally, the distance Rh–C(1) of 1.795(5) Å is significantly shorter than the Rh–C(carbonyl) distances in $[\mathbf{2b}^+]$ (1.843(3) and 1.856(2) Å). Such a shortening can be attributed to a *trans* influence of the ether function.

Considering the solid state structure of the cation $[\mathbf{3}]^+$ it appears that the molecule possesses only a (non crystallographic) C_2 symmetry, the C_2 axis passing through the Rh(1) and O(8) atoms. This is apparently incompatible with the room temperature ^{1}H NMR data, which indicates that the molecule possesses higher symmetry in solution, the methylene groups giving rise to two triplets. As a matter of fact, lowering the temperature of the NMR experiments induces a pro-
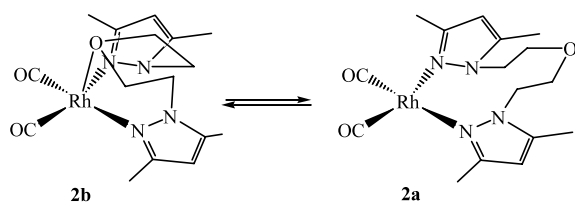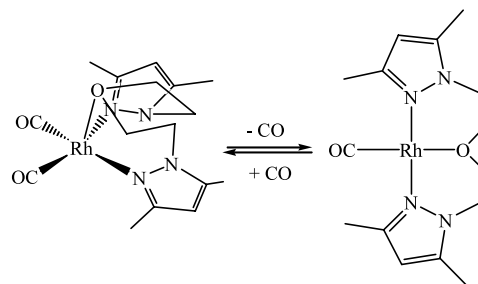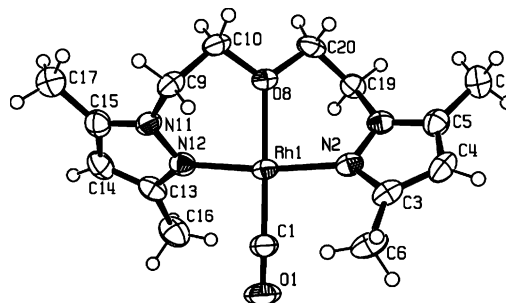

Scheme 2.

Fig. 5. Crystal structure of the cation $[\mathbf{3}]^+$ showing the numbering scheme; ellipsoids are drawn at the 30% probability level.

gressive broadening of the signals of the methylene groups until 230 K, a temperature at which two broad peaks at 3.96 and 4.85 ppm are observed. Further lowering to 190 K induces the appearance of a well-defined AA′BB′ spin systems consistent with the solid-state structure. The coalescence behaviour of the AA′BB′ systems yields an activation energy barrier of 44 kJ mol^{-1} for the observed dynamic process.

This low energy fluxional phenomenon, which renders equivalent the hydrogen atoms inside each methylene group, is certainly a conformational equilibrium of the six-membered chelate ring due to the rocking of the pyrazolyl cycles around the Rh–N bonds without any metal–ligand bond breaking. This has to be contrasted with the fluxional process observed for $[\mathbf{2}]^+$ due to the reversible opening of the Rh–O bond (vide supra) which is a higher energy process.

3. Conclusion

This study illustrates the ability of the ligand $\mathbf{L_1}$ to adopt different conformations and coordination modes when associated with rhodium(I). Notably, a facial κ^3N,N,O mode of coordination has been evidenced in solid state structure of $[Rh(CO)_2(\mathbf{L_1}\text{-}\kappa^3N,N,O)][BF_4]$ $([\mathbf{2b}][BF_4])$ and this constitutes the first example of such a bonding mode for that ligand. $\mathbf{L_1}$ exhibits hemilabile properties as in solution, $[\mathbf{2}]^+$ exists as a mixture of two isomers in which $\mathbf{L_1}$ is either κ^2N,N or κ^3N,N,O-bonded to Rh. Due to the chelating properties

Scheme 1.

of L_1 and its preference for a meridional κ^3N,N,O bonding mode, decarbonylation of $[2]^+$ occurs easily at room temperature to produce $[Rh(CO)(L_1-\kappa^3N,N,O)][BF_4]$ ($[3][BF_4]$). As compared to the ligand L, the ligand L_1 shows a lower propensity to adopt a κ^3 mode of bonding due to the hardest nature of the oxygen of ether function. Indeed, the ligand L adopts a κ^3 mode of bonding in $[Rh(COD)(L-\kappa^3N,N,N)][BF_4]$ in spite of severe steric strains with the COD ligand [1], whereas L_1 shows a κ^2 bonding mode in $[Rh(COD)(L_1-\kappa^2N,N)][BF_4]$ even though the steric strains are expected to be lower due to the longer chain between the pyrazole ring and the heteroatom donor.

4. Experimental

4.1. General remarks

All reactions were carried out under a nitrogen atmosphere with the use of vacuum line and standard Schlenk techniques. All reagents were commercial grade materials and were used without further purification. All solvents were dried and distilled before use by standard methods. The ligand bis[2-(3,5-dimethyl-1-pyrazolyl)ethyl]ether [4] and $[Rh(COD)Cl]_2$ [14] were prepared according to the published procedures. Routine NMR spectra were obtained on Bruker AC200 or AC250 spectrometers. The ^{1}H-NMR variable temperature spectra were recorded on a Bruker DRX500 spectrometer. All chemical shift values (δ) are given in ppm and are referenced with respect to residual protons in the solvent for ^{1}H spectra and to solvent signals for ^{13}C spectra. Elemental analyses (C, N, H) were performed by the staff of the Chemical Analyses Service of the Universitat Autònoma de Barcelona on a Carlo Erba CHNS EA-1108 instrument. Infrared spectra were recorded on a Perkin Elmer 2000 FT spectrophotometer.

4.2. Synthesis of $[Rh(COD)(L_1)][BF_4]$ ($[1][BF_4]$)

$AgBF_4$ (79 mg, 0.40 mmol) was added to a solution of $[Rh(COD)Cl]_2$ (100 mg, 0.20 mmol) in THF (20 ml). The solution was stirred for half an hour at room temperature (r.t.) and light protected. The orange solution turned yellow and AgCl precipitated. The solution was filtered and L_1 (105 mg, 0.40 mmol) was then added. After stirring overnight, the solution was evaporated to dryness and the residue was re-crystallized at $-20\,^\circ$C from a dichloromethane–ether mixture to yield yellow crystals in 87% yield. Anal. Calc. for $C_{22}H_{34}BF_4N_4ORh$ (560.25): C, 47.17; H, 6.07; N, 10.01. Found: C, 46.77; H, 6.11; N, 9.69%. ^{1}H-NMR (CDCl$_3$ solution, 250 MHz) δ: 6.28 [m, $^2J = 15.9$ Hz, $^3J = 2.5$ Hz, $^3J = 11.8$ Hz, 2H, NCHH], 5.93 [s, 2H, CH pyrazole], 4.48 [m, $^2J = 15.9$ Hz, $^3J = 2.4$, $^3J = 0.6$, 2H,

NCHH], 4.26 [m, $^2J = 12.5$ Hz, $^3J = 2.5$ Hz, $^3J = 2.4$ Hz, 2H, OCHH], 4.14 [m, $^2J = 12.5$ Hz, $^3J = 11.8$ Hz, $^3J = 0.6$ Hz, 2H, OCHH], 3.90 [b, 2H, CH cod], 3.71 [b, 2H, CH cod], 2.90 [m, 2H, CHH$_{exo}$ cod], 2.80 [s, 6H, CH$_3$], 2.56 [m, 2H, CHH$_{exo}$ cod], 2.21 [s, 6H, CH$_3$], 1.89 [m, 4H, CHH$_{endo}$ cod]. ^{13}C\{^{1}H\} NMR (CDCl$_3$ solution, 62.9 MHz) δ: 148.4 (CCH$_3$), 142.9 (CCH$_3$), 108.9 (CH pyrazole), 84.4 (d, $J_{Rh-C} = 12$ Hz, =CH), 83.7 (d, $J_{Rh-C} = 12$ Hz, =CH), 72.9 (OCH$_2$), 54.0 (NCH$_2$), 30.6–30.1 (CH$_2$ cod), 16.0 (CH$_3$), 11.9 (CH$_3$).

4.3. Synthesis of $[Rh(CO)_2(L_1)][BF_4]$ ($[2][BF_4]$)

Carbon monoxide was bubbled for 2 h through a solution of $[1][BF_4]$ (100 mg) dissolved in dichloromethane (20 ml). The yellow solution turned dark yellow. The solution was then evaporated to dryness in vacuum to leave a dark yellow powder, which was re-crystallized in a dichloromethane–ether mixture under a CO atmosphere by cooling at $-20\,^\circ$C. Orange crystals corresponding to the isomer $[2b]^+$ were obtained in 60% yield. Anal. Calc. for $C_{16}H_{22}BF_4N_4O_3Rh$ (508.10): C, 37.82; H, 4.33; N, 11.03. Found: C, 37.57; H, 4.49; N, 10.43%. IR (CH$_2$Cl$_2$ solution) v(CO): isomer $[2a]^+$: 2105(w), 2042(w) cm^{-1}; isomer $[2b]^+$: 2090(s), 2022(s) cm^{-1}. ^{1}H NMR ((CD$_3$)$_2$CO solution at 240 K, 500 MHz) δ: 6.26 (s, 2H, CH pyrazole), 4.87 [dd, $^2J = 15.8$ Hz, $^3J = 9.5$ Hz, 2H, NCHH], 4.21 [d, $^2J = 12.0$ Hz, 2H, OCHH], 4.09 [d, $^2J = 15.8$ Hz, 2H, NCHH], 3.99 [dd, $^2J = 12.0$ Hz, $^3J = 9.5$ Hz, 2H, OCHH], 2.48 [s, 6H, CH$_3$], 2.38 [s, 6H, CH$_3$]. ^{13}C\{^{1}H\} NMR ((CD$_3$)$_2$CO solution, 62.9 MHz) δ: 182.8 (d, $J_{Rh-C} = 70.5$ Hz, CO), 152.4 (CCH$_3$), 145.9 (CCH$_3$), 108.9 (CH pyrazole), 71.4 (OCH$_2$), 51.2 (NCH$_2$), 16.2 (CH$_3$), 12.6 (CH$_3$).

4.4. Synthesis of $[Rh(CO)(L_1)][BF_4]$ ($[3][BF_4]$)

$[2][BF_4]$ was crystallized at $-20\,^\circ$C in a dichloromethane–ether mixture under N$_2$. Crystals of $[3][BF_4]$ were obtained as yellow needles. Anal. Calc. for $C_{15}H_{22}BF_4N_4O_2Rh$ (480.09): C, 37.52; H, 4.59; N, 11.67. Found: C, 37.30; H, 4.46; N, 11.24%. IR (CH$_2$Cl$_2$ solution) v(CO): 1994(s) cm^{-1}. ^{1}H NMR ((CD$_3$)$_2$CO solution, 200 MHz) δ: 6.22 [s, 2H, CH pyrazole], 4.92 [t, $^3J = 4.5$ Hz, 4H, NCH$_2$], 4.09 [t, $^3J = 4.5$ Hz, 4H, OCH$_2$], 2.42 [s, 6H, CH$_3$], 2.37 [s, 6H, CH$_3$]. (CD$_2$Cl$_2$ solution at 190 K, 500 MHz) δ: 6.03 [s, 2H, CH pyrazole], 4.83 [dd, $^2J = 15.7$ Hz, $^3J = 11.6$ Hz, 2H, NCHH], 4.50 [d, $^2J = 15.7$ Hz, 2H, NCHH], 3.98 [d, $^2J = 9.5$ Hz, 2H, OCHH], 3.79 [dd, $^2J = 9.5$ Hz, $^3J = 11.6$ Hz, 2H, OCHH], 2.31 [s, 6H, CH$_3$], 2.30 [s, 6H, CH$_3$] ^{13}C\{^{1}H\} NMR ((CD$_3$)$_2$CO solution, 62.9 MHz) δ: 186.2 (d, $J_{Rh-C} = 89.3$ Hz, CO), 152.7 (CCH$_3$), 144.5 (CCH$_3$), 108.4 (CH pyrazole), 73.1 (OCH$_2$), 48.6 (NCH$_2$), 15.3 (CH$_3$), 11.5 (CH$_3$).

4.5. X-ray crystallographic study

Crystals of [**1**][BF$_4$], [**2b**][BF$_4$] and [**3**][BF$_4$] suitable for X-ray diffraction were obtained through re-crystallization from dichloromethane–ether mixtures (under a CO atmosphere for [**2b**][BF$_4$]). Data were collected on a STOE IPDS diffractometer at 160 K for [**1**][BF$_4$] and [**2b**][BF$_4$] and at 293 K for [**3**][BF$_4$]. Full crystallographic data for the three complexes are gathered in Table 2. All calculations were performed on a personal computer using the WINGX system [15]. The structures were solved by using the SIR-92 program [16], which revealed in each instance the position of most of the non-hydrogen atoms. All remaining non-hydrogen atoms were located by the usual combination of full matrix least-squares refinement and difference electron density syntheses by using the SHELXS-97 program [17]. Atomic scattering factors were taken from the usual tabulations [18]. Anomalous dispersion terms for Rh atoms were included in Fc [19]. All non-hydrogen atoms were allowed to vibrate anisotropically. All the hydrogen atoms were set in idealized position (R$_3$CH, C–H = 0.96 Å; R$_2$CH$_2$, C–H = 0.97 Å; RCH$_3$, C–H = 0.98 Å; C(sp2)–H = 0.93 Å; U$_{iso}$ 1.2 or 1.5 times greater than the U$_{eq}$ of the carbon atom to which the hydrogen atom is attached).

Complex [**1**][BF$_4$] was found to crystallize with two independent pairs of ions per unit cell. The structure was best refined considering a racemic twin with a 0.41268/0.58732 relative contribution of the twin components. In addition, one of the BF$_4$ counter-anion was found to be disordered; a suitable model was found considering a rotation of ca. 30° of the F$_4$ tetrahedron around one of the B–F axis. In the structure of complex [**3**][BF$_4$] also the BF$_4$ counter-anion was found to be disordered; a suitable model was refined considering a head-to-tail arrangement of pairs of BF$_4$ units sharing a face of the F$_4$ tetrahedrons along an axis parallel to *a* axis. In addition, two strong residual peaks were observed in the finals difference Fourier maps; these peaks were finally attributed to water molecule statistically distributed over two different sites in channels parallel to the *a* axis.

5. Supplementary material

Crystallographic data for the structural analysis have been deposited with the Cambridge Crystallographic Data Centre, CCDC nos. 208789–208791 for compounds [**1**][BF4], [**2b**][BF$_4$] and [**3**][BF$_4$], respectively. Copies of this information may be obtained free of

Table 2
Crystal data for [**1**][BF$_4$], [**2b**][BF$_4$] and [**3**][BF$_4$]

Compound	[**1**][BF$_4$]	[**2b**][BF$_4$]	[**3**][BF$_4$]
Empirical formula	C$_{44}$H$_{68}$B$_2$F$_8$N$_8$O$_2$Rh$_2$	C$_{32}$H$_{44}$B$_2$F$_8$N$_8$O$_6$Rh$_2$	C$_{15}$H$_{22}$BF$_4$N$_4$O$_3$Rh
Molecular weight (g)	1120.50	1016.19	480.09
Temperature (K)	160(2)	160(2)	293(2)
Wavelength (Å)	0.71073	–	–
Crystal system	Orthorhombic	Triclinic	Triclinic
Space group	$Pca2_1$ (no. 29)	$P\bar{1}$ (no. 2)	$P\bar{1}$ (no. 2)
Unit cell dimensions			
a (Å)	27.684(5)	8.1696(12)	4.6776(5)
b (Å)	7.942(5)	9.9445(15)	12.4521(15)
c (Å)	21.712(5)	12.8477(19)	17.720(2)
α (°)	90	87.839(18)	97.584(14)
β (°)	90	89.683(17)	92.555(13)
γ (°)	90	77.286(17)	99.906(13)
V (Å^3)	4774(3)	1017.5(3)	1005.4(2)
Z	4	2	2
D_{calc} (g cm^{-3})	1.559	1.658	1.639
μ (mm^{-1})	0.769	0.900	0.908
$F(000)$	2304	512	500
θ Range (°)	2.56–26.24	2.10–26.09	2.17–26.04
Index ranges	$-34 \leq h \leq 34$, $-9 \leq k \leq 9$, $-26 \leq l \leq 26$	$-9 \leq h \leq 10$, $-12 \leq k \leq 12$, $-15 \leq l \leq 15$	$-5 \leq h \leq 5$, $-15 \leq k \leq 15$, $-21 \leq l \leq 21$
Reflections collected	36028	8815	9936
Independent reflections	9369 [$R_{int} = 0.0539$]	3621 [$R_{int} = 0.0223$]	3668 [$R_{int} = 0.0412$]
Completeness to θ_{max} (%)	98.4	89.7	91.3
Refinement method	Full-matrix least-squares on F^2	Full-matrix least-squares on F^2	Full-matrix least-squares on F^2
Data/restrains/parameters	9335/73/631	3621/0/266	3640/70/275
Goodness of fit on F^2	1.058	0.999	1.049
R [$I > 2\sigma(I)$]	$R_1 = 0.0493$, $wR_2 = 0.1240$	$R_1 = 0.0261$, $wR_2 = 0.0655$	$R_1 = 0.0448$, $wR_2 = 0.1136$
R (all data)	$R_1 = 0.0509$, $wR_2 = 0.1263$	$R_1 = 0.0273$, $wR_2 = 0.0662$	$R_1 = 0.0576$, $wR_2 = 0.1200$
Residual electron density (e Å^{-3})	2.497 and -0.826	0.842 and -0.614	1.120 and -0.568

charge from The Director, CCDC, 12 Union Road, Cambridge CB2 1EZ, UK (Fax: +44-1223-336033; e-mail: deposit@ccdc.cam.ac.uk or www: http://www.ccdc.cam.ac.uk).

References

[1] R. Mathieu, G. Esquius, N. Lugan, J. Pons, J. Ros, Eur. J. Inorg. Chem. (2001) 2683.
[2] B. Lupo, M. Gál, G. Tarrago, Bull. Soc. Chim. Fr. 11–12 (1984) 464.
[3] B. Lupo, G. Tarrago, Bull. Soc. Chim. Fr. 11–12 (1984) 473.
[4] T.N. Sorrell, M.R. Malachowski, Inorg. Chem. 22 (1983) 1883.
[5] C. Dowling, V.J. Murphy, G. Parkin, Inorg. Chem. 35 (1996) 2415.
[6] E.A.H. Griffith, N.G. Charles, K. Lewinski, E.L. Amma, P.F. Rodesiler, Inorg. Chem. 26 (1987) 3983.
[7] P.H.M. Budzelaar, 'gNMR ver. 4.0' Ivory Soft, Cherwell Scientific, Oxford, 1997.
[8] L.A. Oro, M. Esteban, R.M. Claramunt, J. Elguero, C. Foces-Foces, F.H. Cano, J. Organomet. Chem. 276 (1984) 79.
[9] A. Jacobi, G. Huttner, E. Winterhalter, J. Organomet. Chem. 571 (1998) 231.
[10] M. Akita, K. Ohta, Y. Takahashi, S. Hikichi, Y. Moro-oka, Organometallics 16 (1997) 4121.
[11] M.C. Keyes, V.G. Young, W.B. Tolman, Organometallics 15 (1996) 4133.
[12] T. Yoshida, T. Okano, S. Otsuka, I. Miura, T. Kubota, K. Kafuku, K. Nakatsu, Inorg. Chim. Acta 100 (1985) 7 (and references therein).
[13] N.W. Alcock, J.B. Brown, J.C. Jeffery, J. Chem. Soc. Dalton Trans. (1976) 583.
[14] G. Giordano, R.H. Crabtree, Inorg. Synth. 32 (1990) 837.
[15] L.J. Farrugia, J. Appl. Crystallogr. 32 (1999) 837.
[16] A. Altomare, G. Cascarano, G. Giacovazzo, A. Guagliardi, J. Appl. Crystallogr. 26 (1993) 343.
[17] G.M. Sheldrick, SHELXS-97, SHELXL-97, CIFTAB – Programs for Crystal Structure Analysis (Release 97-2), Institüt für Anorganische Chemie der Universität, Tammanstrasse 4, D-3400 Göttingen, Germany, 1998.
[18] (a) D.T. Cromer, J.T. Waber, International Tables for X-ray Crystallography (Table 22B), vol. 4, Kynoch Press, Birmingham, UK, 1974;
(b) R.F. Stewart, E.R. Davidson, W.T. Simpson, J. Chem. Phys. 42 (1965) 3175;
(c) T. Hahn (Ed.), International Tables for Crystallography, vol. A, Kluwer Academic Publishers, Dordrecht, The Netherlands, 1995.
[19] D.T. Cromer, J.T. Waber, International Tables for X-ray Crystallography (Table 2.3.1), vol. 4, Kynoch Press, Birmingham, UK, 1974.